

Table II

atom	orbital	$H_{ij}$ , eV	exponent
Be	2s	-10.00	1.25
	2p	-6.00	1.25
C	2s	-21.4	1.625
	2p	-11.4	1.625
O	2s	-32.3	2.275
	2p	-14.8	2.275
Cl	3s	-30.0	2.033
	3p	-15.0	2.033
Si	3s	-17.3	1.383
	3p	-9.2	1.383
Pd	5s	-9.57	2.19
	5p	-3.43	2.15
	4d	-14.07	5.98 (0.5265), 2.613 (0.6372) <sup>a</sup>

<sup>a</sup> Double- $\zeta$  wave function; coefficients in parentheses.

about because of our elimination of "ligand-ligand" interactions in the calculation of the local energetic contribution at the cationic site. This is somewhat artificial since the geometries of free molecules are set by a combination of central-atom-ligand and ligand-ligand effects. In other words, the matrix effect, described in this paper, includes steric effects between the ligands that a molecular chemist would take for granted. On the other hand, there are many more close anion-anion contacts in the crystal, and their importance is correspondingly greater. An interesting result still is that the observed arrangement is one that concurrently satisfies local geometrical (often tetrahedral) and matrix requirements. We have described a similar situation for some molecular fragments in ref 1a. There we demonstrate an excellent correlation between the one-electron orbital energy associated with central-atom-ligand interaction and the energetics of ligand-ligand repulsions using the points-on-a-sphere model.<sup>19b</sup> The physical reasoning behind such a correspondence has yet to be elucidated.

Given the energetic importance of the matrix, the use of numerical data gleaned from calculations on molecular fragments needs to be interpreted carefully. The qualitative aspects of bond length/bond angle relationships, and indeed of the geometrical

details of silicate structures elucidated so beautifully by Gibbs and co-workers<sup>2,3,20</sup> will clearly still hold, but the use of potential function data, derived from systems where only a fraction of the close contacts of the solid are included, may well not be a good way to quantitatively model either bulk properties or the energy difference between systems with very different crystal structures. A complicating factor here too is that the stoichiometry of the fragment chosen is, of necessity, not that of the crystal itself.

**Acknowledgment.** This research was supported by the National Science Foundation, Grant Nos. NSF DMR 8019741 and NSF DMR 8216892. D.C.C. was also supported by a generous grant from the Richter Fund.

#### Appendix

All of the calculations described in this paper used the extended Hückel method both for the molecular orbital calculations on the fragments torn from the crystal lattice and for the tight-binding computations on the crystalline materials. The parameters are given in Table II.

All the calculations involving geometrical deformations maintained constant nearest-neighbor anion-cation distances. These were as follows: Be-O, 1.60 Å; Pd-O, 1.95 Å; Si-O, 1.62 Å for quartz and tridymite, 1.70 Å for silica-w (this is close to the average distance in the molecule **8**<sup>24</sup>), and 1.77 Å for stishovite (this is the average of the symmetry-inequivalent distances in the crystal<sup>25</sup>); Pd-Cl, 2.309 Å. Sufficient  $k$  points were included to achieve energetic convergence. For the calculations on  $\beta$ -quartz, for example, a set of eight points within the irreducible wedge of the hexagonal Brillouin zone was found to be adequate. The lattice sums of the tight-binding calculations were invariably over two unit cells in all three directions. In two of the calculations on  $\beta$ -quartz, however, no interactions were included beyond 3 Å, in an attempt to gauge the importance of direct silicon-silicon interactions.

**Registry No.** BeO, 1304-56-9; PdCl<sub>2</sub>, 7647-10-1; PtS, 12038-20-9; PtO, 12035-82-4; PdO, 1314-08-5; SiO<sub>2</sub>, 7631-86-9; cooperite, 12197-03-4;  $\beta$ -tridymite, 15468-32-3;  $\beta$ -quartz, 14808-60-7; stishovite, 13778-37-5.

Contribution from the Dipartimento di Chimica Generale, Università di Pavia, 27100 Pavia, Italy

## Formation of a Trivalent Silver Tetraaza Macrocyclic Complex in Aqueous Solution: Hydrolytic Tendencies and Interaction with the Sulfate Ion

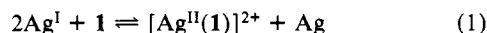
MARIA PESAVENTO, ANTONELLA PROFUMO, TERESA SOLDI, and LUIGI FABBRIZZI\*

Received January 18, 1985

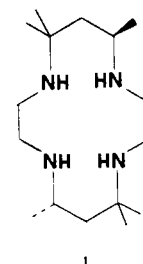
The Ag<sup>II</sup> complex with the tetraaza macrocycle **1** in aqueous solution undergoes a reversible one-electron-oxidation process to give an authentic Ag<sup>III</sup> species. The Ag<sup>III</sup>/Ag<sup>II</sup> redox couple potential (0.835 V vs. Ag/AgCl) is affected by variation of the acidity of the solution, indicating that the Ag<sup>III</sup>(**1**) complex behaves as a fairly strong acid ( $pK = 2.6$ ). The positive value of the reaction entropy for the [Ag<sup>III</sup>(**1**)]<sup>3+</sup>/[Ag<sup>II</sup>(**1**)]<sup>2+</sup> redox couple, measured with a nonisothermal method, indicates that the water molecules must be present in the coordination sphere of the trivalent complex. Presence of sulfate in solution stabilizes the Ag<sup>III</sup> complex due to the formation of a 1:1 adduct.

### Introduction

The disproportionation reaction of Ag<sup>+</sup>, eq 1, in the presence of a 14-membered tetraaza macrocycle such as **1** to give a silver mirror and a yellow solution of the Ag<sup>II</sup> tetraaza macrocyclic complex, was independently discovered by Allred<sup>1</sup> and Barefield.<sup>2</sup>



This distinctive aspect of the coordination chemistry of silver reflects the tendency of cyclic tetraaza ligands to establish strong in-plane metal-nitrogen interactions, according to a tetragonal stereochemistry: the transition-metal ion Ag<sup>II</sup> (electronic con-



figuration d<sup>9</sup>) profits to such a large extent from this effect that the Ag<sup>I</sup>/Ag<sup>II</sup> oxidation process can be accomplished even by a smooth oxidizing agent such as Ag<sup>I</sup>.

(1) Kestner, M. O.; Allred, A. L. *J. Am. Chem. Soc.* **1972**, *94*, 71.

(2) Barefield, E. K.; Mocella, M. T. *Inorg. Chem.* **1973**, *12*, 78.

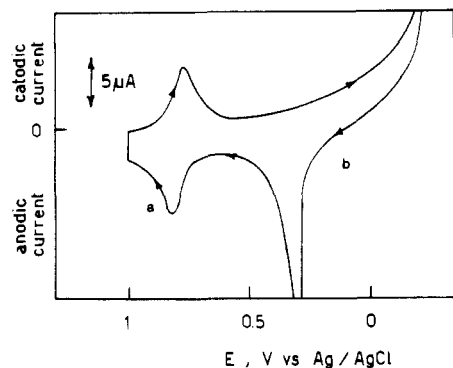


**Figure 1.** Cyclic voltammogram profile for an aqueous solution  $10^{-3}$  M in  $\text{Ag}(\text{I})(\text{ClO}_4)_2$ , adjusted at pH 2 with  $\text{HClO}_4$  and to 0.1 M ionic strength with  $\text{NaClO}_4$ . Working electrode, platinum microsphere, potential scan rate,  $100 \text{ mV s}^{-1}$ .

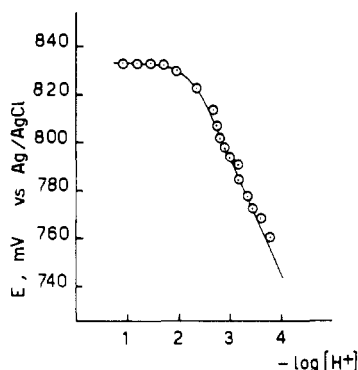


**Figure 2.** Dependence of the  $E_{1/2}([\text{Ag}^{\text{III}}(\text{I})]^{3+}/[\text{Ag}^{\text{II}}(\text{I})]^{2+})$  value on the acidity of the solution. Ionic strength was adjusted to 0.1 M with  $\text{NaClO}_4$ .

The molecular structure of the  $\text{Ag}^{\text{II}}(\text{I})(\text{NO}_3)_2$  complex has been reported,<sup>3</sup> showing a square-planar array of amine nitrogen atoms at an average distance of 2.16 Å; nitrate oxygen atoms occupy the apical positions of the axially distorted octahedron, according to a stereochemistry well familiar to corresponding  $\text{Cu}^{\text{II}}$  tetramine complexes.

A further interesting aspect of the redox chemistry of silver tetraaza macrocyclic complexes was disclosed by Barefield,<sup>2</sup> who described the one-electron oxidation of the  $[\text{Ag}^{\text{II}}(\text{macrocycle})]^{2+}$  complex in anhydrous acetonitrile solution, performed both electrochemically (with a platinum anode) and chemically (with  $\text{NOBF}_4$ ), to give an  $\text{Ag}^{\text{III}}$  species (the authenticity of the  $\text{Ag}^{\text{III}}$  state was demonstrated by the complete disappearance, on oxidation, of the ESR signal of the  $\text{Ag}^{\text{II}}$  complex). In this sense, the behavior of the  $\text{Ag}^{\text{III}}$  tetraaza macrocyclic complexes is similar to that of  $\text{Ni}^{\text{II}}$  analogues, which undergo one-electron oxidation to form stable  $\text{Ni}^{\text{III}}$  species.<sup>4,5</sup> Interestingly, the electrode potentials in acetonitrile solution for the  $\text{M}^{\text{III}}/\text{M}^{\text{II}}$  redox couple for nickel and silver tetraaza macrocyclic complexes exhibit similar values. More recently, it has been shown that  $\text{Ni}^{\text{III}}$  tetraaza macrocyclic complexes can be obtained also in water, where they are stable in the acidic pH range.<sup>6</sup>

Furthermore, an interesting chemistry of  $\text{Ni}^{\text{III}}$  tetraaza macrocyclic complexes in aqueous solution has been developed with a special regard to their interaction with inorganic anions.<sup>7</sup> The above considerations prompted us to explore the existence of an aqueous chemistry also for silver(III) tetraaza macrocyclic complexes.

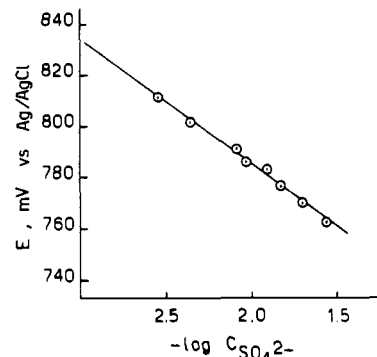


**Figure 3.** Dependence of the  $([\text{Ag}^{\text{III}}(\text{I})]^{3+}/[\text{Ag}^{\text{II}}(\text{I})]^{2+})$  value upon the concentration of the sulfate ion of an acidic solution ( $-\log [\text{H}^+] = 1.8$ ). Ionic strength of the solution was adjusted to 0.1 M with  $\text{NaClO}_4$ .

In this connection, we have investigated the redox behavior of the silver(II) complex with the fully saturated tetraaza macrocycle *meso*-5,7,7,12,14,14-hexamethyl-1,4,8,11-tetraazacyclotetradecane (**1**).

### Experimental Section

All reagents were of analytical grade.  $\text{Ag}^{\text{II}}(\text{I})(\text{ClO}_4)_2$  has been obtained according to Barefield.<sup>2</sup> Polarographic and voltammetric measurements were carried out with a Metrohm Polarecord E 506 apparatus by using a three-electrode system consisting of an  $\text{Ag}/\text{AgCl}$  reference electrode and either a platinum or a glassy-carbon working electrode.  $-\log [\text{H}^+]$  measurements have been performed by means of an Orion Model 701 A potentiometer using a calibrated glass electrode; bulk anodic oxidation of the complexes was carried out with an AMEL Model 550 potentiostat with an AMEL Model 558 RM integrator with use of either platinum gauze or a mercury pool as working electrode,  $\text{Ag}/\text{AgCl}$ ,  $\text{KCl}$  in  $\text{NaNO}_3$  salt bridge as a reference electrode, and a platinum coil dipped in a  $\text{Na}_2\text{SO}_4$  solution as counter electrode.

All the experiments were performed in a cell thermostated at  $25 \pm 0.05$  °C by means of an Endocal RTE 9B apparatus.

### Results and Discussion

The  $\text{Ag}^{\text{II}}(\text{I})(\text{ClO}_4)_2$  complex dissolves in water to give a yellow solution that is indefinitely stable, as shown by the persistence of the absorption band in the visible region ( $\lambda_{\text{max}} = 350 \text{ nm}$ ; molar extinction coefficient = 3.85 log units). pH titration, performed by adding standard base to an acidified solution of  $[\text{Ag}(\text{I})]^{2+}$  indicated that the  $\text{Ag}(\text{II})$  complex does not exhibit any hydrolytic tendency in the pH range 2–6. On addition of further base (pH > 10), the yellow solution decolorizes and some turbidity forms, probably due to decomposition. Cyclic voltammetry investigation of an acidic solution of  $[\text{Ag}(\text{I})]^{2+}$ , performed by using a platinum microsphere as well as a glassy-carbon working electrode (see Figure 1), disclosed in the reduction scan an irreversible peak at  $-0.1$  to  $-0.2 \text{ V}$  vs.  $\text{Ag}/\text{AgCl}$ , followed in the reverse scan by an anodic stripping peak (see Figure 1, part B), which suggests demetalation of the complex and simultaneous reduction to silver metal. The controlled-potential-coulometry experiment, using a mercury cathode, indicated the consumption of 2 mol of electrons/mol of  $\text{Ag}^{\text{II}}$  complex. On the other hand, the CV oxidation scan (see Figure 2, part A), showed a reversible one-electron response (separation of anodic and cathodic peaks  $\Delta p = 60 \text{ mV}$  in the potential scan rate range  $10$ – $200 \text{ mV s}^{-1}$ ; ratio of anodic and cathodic peaks,  $i_c/i_a = 1$ ) which was ascribed to a reversible pH-dependent  $\text{Ag}^{\text{III}}/\text{Ag}^{\text{II}}$  redox change. The ac investigation disclosed a symmetric profile, whose peak half-width was 90 mV. On electrolysis the solution turned pale yellow: no attempts were made to isolate the trivalent silver complex.<sup>8</sup> The half-potential exhibits a constant value ( $0.835 \pm 0.003$  vs.  $\text{Ag}/\text{AgCl}$ ), in the  $-\log [\text{H}^+]$  range 1.0–1.8. Corresponding values of  $E_{1/2}$  ( $\text{Ag}^{\text{III}}/\text{Ag}^{\text{II}}$ ) have been obtained from CV profiles (glassy carbon working electrode).

Figure 2 shows the pH dependence of  $E_{1/2}$  values in the pH

(3) Mertes, K. B. *Inorg. Chem.* **1978**, *17*, 49.

(4) LoVecchio, F. V.; Gore, E. S.; Busch, D. H. *J. Am. Chem. Soc.* **1974**, *96*, 3110.

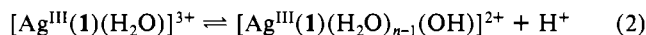
(5) Bencini, A.; Fabbrizzi, L.; Poggi, A. *Inorg. Chem.* **1981**, *20*, 2544.

(6) Cohen, H.; Kirschenbaum, L. J.; Zeigerson, E.; Jacobi, M.; Fuchs, E.; Ginzburg, G.; Meyerstein, D. *Inorg. Chem.* **1979**, *18*, 276.

(7) Haines, R. I.; McAuley, A. *Inorg. Chem.* **1976**, *15*, 1502.

(8) The coulometry experiment, performed by imposing at the working electrode (platinum gauze) a potential 200 mV greater than  $E_{1/2}$ , confirmed the one-electron stoichiometry of the oxidation process.

range 1–4. In the more acidic region (up to pH 2) the potential remains constant; at pH higher than 2 the  $E_{1/2}$  value decreases linearly with a slope of 59 mV  $(-\log [H^+])^{-1}$ . This behavior is consistent with equilibrium 2, which involves the hydrolysis of



trivalent complex: the proton is presumably extruded from a coordinated solvent molecule. It should be noted that above pH 4 the CV response becomes irreversible.

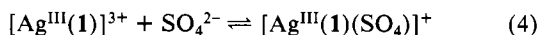
The constant of equilibrium 2 can be calculated from eq 3, where  $E_{1/2}^*$  is the potential value measured in the strongly acidic region ( $1.0 \leq \log [H^+] \leq 1.8$ ). Least-squares analysis of data

$$E_{1/2} = E_{1/2}^* + \log \frac{[H^+]}{[H^+] + K_h} \quad (3)$$

shown in Figure 2 gave a  $pK_h$  value of  $2.6 \pm 0.1$ , indicating that the  $[Ag^{III}(1)]^{3+}$  complex behaves as a fairly strong acidic cation, considerably more acidic for instance, than the analogue  $[Ni^{III}(1)]^{3+}$  for which a  $pK_h$  value of 3.9 has been measured.<sup>6</sup>

**Interaction with the Sulfate Ion.**  $SO_4^{2-}$  binds fairly strongly  $[Ni^{III}(1)]^{3+}$  in aqueous solution, making considerably easier the attainment of the trivalent state of nickel in a sulfate salt solution.<sup>6</sup> The silver complex investigated here displays a similar behavior, the  $E_{1/2}(Ag^{III}/Ag^{II})$  value being seriously affected by  $SO_4^{2-}$  concentration.

Experiments have been carried out, keeping the  $-\log [H^+]$  value constant (performing measurements at selected values in the range 1.0–2.5) and varying  $SO_4^{2-}$  concentration (the ionic strength being correspondingly adjusted to 0.1 M with  $NaClO_4$ ). Figure 3 reports the plot of  $E_{1/2}(Ag^{III}/Ag^{II})$  values vs.  $-\log C_{SO_4^{2-}}$ . A linear dependence is displayed, with a slope of  $-59$  mV  $(\log C_{SO_4^{2-}})^{-1}$ . This behavior is consistent with equilibrium 4. The binding



constant of sulfate ( $K$ ) can be obtained from eq 5, where  $\alpha_{H^+} =$

$$E_{1/2} = E_{1/2}^* + 0.059 \log \frac{[H^+]}{(1/\alpha_{H^+}[H^+]) + KC_{SO_4^{2-}}\alpha_{SO_4^{2-}}} \quad (5)$$

$[H^+]/([H^+] + K_h)$ ,  $\alpha_{SO_4^{2-}} = K_{A_2}/([H^+] + K_{A_2})$ , and  $K_{A_2}$  is the stepwise dissociative constant of sulfuric acid, relative to the  $HSO_4^-/SO_4^{2-}$  equilibrium. The value of  $K$  calculated from eq 5 (2.9 log units) indicates that  $SO_4^{2-}$  has a considerably lower affinity toward  $[Ag^{III}(1)]^{3+}$  than toward  $[Ni^{III}(1)]^{3+}$  (4.5 log units).

**Stereochemistry of the  $Ag^{II}$  Macrocyclic Complex and Reaction Entropies for the  $Ag^{III}/Ag^{II}$  Redox Couple.** The  $[Ag^{III}(1)]^{3+}$  ion is ESR silent, from which a  $d^8$  (presumably low-spin) electronic configuration has been deduced. One of the best known low-spin  $d^8$  cations is  $Ni^{II}$ , and its tendency to give square-planar complexes with tetramine ligands is well documented: advantages of this type of stereochemistry can be fully justified by using CFSE arguments. A square planar stereochemistry has been hypothesized also for  $Cu^{III}$  complexes with tetraaza macrocycles,<sup>9,10</sup> but no direct evidence for this coordinative arrangement has been reported until now. However, our findings suggest that extrapolation of the Ni and Cu stereochemistry to the  $Ag^{III}$  macrocyclic complex may not be totally correct: in fact, the acid–base behavior of the  $[Ag^{III}(1)]^{3+}$  complex suggests that at least one water molecule is present in the coordination sphere of the complex, and judging from the values of  $pK_A$ , it must be bound more tightly than in the case of the  $Ni^{III}$  analogue; it should also be recalled that in the case of  $Ni^{III}$  a trans octahedral stereochemistry has been ascertained,<sup>4,5</sup> the solvent molecules occupying the apical

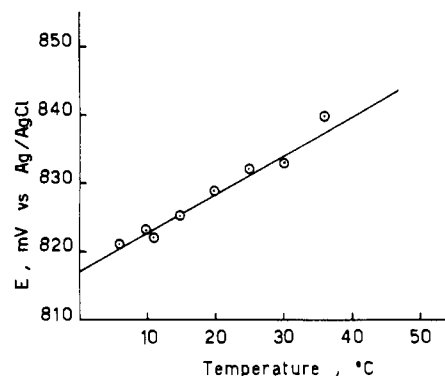


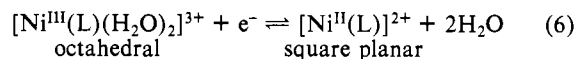
Figure 4. Dependence of the  $E_{1/2}([Ag^{III}(1)]^{3+}/[Ag^{II}(1)]^{2+})$  value upon temperature (5–37 °C). The slope gives the entropy value of the redox half-reaction entropy ( $+13.3 \pm 0.5$  cal  $deg^{-1}$   $mol^{-1}$ ).

positions of the elongated octahedron. Further evidence of the presence of water molecules in the coordination sphere of the Ag complex is given by the study of the temperature dependence of the  $E_{1/2}(Ag^{III}/Ag^{II})$  value with a nonisothermal cell. It is known that the temperature coefficient of the electrode potential  $E^\circ$  is linearly related to the entropy change of the half-cell reaction involving the redox couple of interest, where a nonisothermal configuration is used.

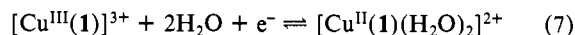
$$\left( \frac{dE}{dT} \right)_{\text{nonisothermal}} = \frac{S^\circ_{\text{red}} - S^\circ_{\text{ox}}}{nF}$$

A successful application of this method has been recently reported by Margerum for the  $Ni^{III}/Ni^{II}$  and  $Cu^{III}/Cu^{II}$  redox changes in complexes with oligopeptides.<sup>12</sup>

The reaction entropy for the  $Ni^{III}/Ni^{II}$  couple was found to be positive (9–11 cal  $mol^{-1}$   $K^{-1}$ ), and this was ascribed to the increase of the number of particles in the reduction process due to the liberation of two water molecules, according to equilibrium 6. On



the contrary, for the  $Cu^{III}/Cu^{II}$  redox change a negative value of  $\Delta S$  has been determined (which ranges from 13 to 20 cal  $K^{-1}$   $mol^{-1}$  in the series of oligopeptides investigated),<sup>12</sup> and this was attributed to a decrease of translational entropy due to the disappearance of solvent molecules in redox equilibrium 7. We have



studied the temperature dependence of the  $Ag^{III}(1)/Ag^{II}(1)$  redox couple potential, using the  $AC_1$  technique in the temperature range 5–37 °C. The voltammetric profiles showed reversible character in the temperature range investigated. A plot of  $E$  vs. temperature was linear (see Figure 4), and the slope corresponded to a value of  $+13.3 \pm 0.5$  cal  $deg^{-1}$   $mol^{-1}$ .

Present results strongly suggest that water molecules are released during the  $Ag^{III}/Ag^{II}$  reduction half-reaction and that they must be present in the coordination sphere of the trivalent complex. On this assumption, the reaction of  $[Ag^{III}(1)]^{3+}$  with  $SO_4^{2-}$  must be considered as a substitution of a water molecule. The strong  $Ag^{III}-OH_2$  interaction, inferred from the strong acid tendencies, may explain the fact that binding of  $SO_4^{2-}$  is considerably less favored than in the case of the  $Ni^{III}$  analogue.

**Acknowledgment.** We thank the Ministry of Public Education for financial support.

**Registry No.**  $[Ag^{II}(1)]^{2+}$ , 48186-19-2;  $[Ag^{III}(1)]^{3+}$ , 48186-20-5;  $Ag(1)(ClO_4)_2$ , 41777-44-0;  $SO_4^{2-}$ , 14808-79-8;  $NaClO_4$ , 7601-89-0.

(9) Olson, D. C.; Vasilevskis, J. *Inorg. Chem.* **1971**, *10*, 463.

(10) Fabbri, L.; Poggi, A.; Zanello, P. *J. Chem. Soc., Dalton Trans.* **1983**, 2191.

(11) Diaddario, L. L.; Robinson, W. R.; Margerum, D. W. *Inorg. Chem.* **1983**, *22*, 1021.

(12) Youngblood, M. P.; Margerum, D. W. *Inorg. Chem.* **1980**, *19*, 3068.